Research Article

# Lubricant Evaluation Technique for Single Point Incremental Forming Process

Khompee Limpadapun and Ramil Kesvarakul
Department of Production Engineering, Faculty of Engineering, King Mongkut's University of Technology North Bangkok, Bangkok, Thailand

Yingyot Aue-u-lan
Material Manufacturing and Surface Engineering Research Center (MaSE), Materials and Production Engineering Program, The Sirindhorn International Thai-German Graduate School of Engineering (TGGS), King Mongkut's University of Technology North Bangkok, Bangkok, Thailand

Thanasan Intarakumthornchai*
Department of Industrial Engineering, Faculty of Engineering, King Mongkut's University of Technology North Bangkok, Bangkok, Thailand

* Corresponding author. E-mail: thanasan.i@eng.kmutnb.ac.th DOI: 10.14416/j.asep.2021.11.009
Received: 7 May 2021; Revised: 7 July 2021; Accepted: 3 August 2021; Published online: 24 November 2021
© 2021 King Mongkut's University of Technology North Bangkok. All Rights Reserved.

**Abstract**
Single-Point Incremental Forming (SPIF) is a highly flexible dieless forming process suitable for small batch production. The higher the feed rate and tool rotational speed, the higher the production rate will be. Therefore, the selection of the suitable lubricant is a key important factor to maintain the formability of the material when increasing the feed rate and tool rotational speed. This paper proposes the technique to evaluate and later on select the proper lubricant for these conditions. This technique was divided into two phases; 1) screening, and 2) stabilization. The screening phase is a quick method for preliminary selection of the lubricants. The stabilizing phase is a step to evaluate the reliability and ensure efficiency of the lubricant throughout the process because of the significant increase in forming temperature, which directly effects lubricant's performance. the performance of the lubricant. Two types of lubricants, namely solid (Graphite) and liquid (Callington Calform NF-206), lubricants mixed with the base oil (coconut oil) at different ratios were tested. The cold rolled hot-dipped zinc-coated steel sheet with a thickness of 0.176 mm. and wall angles of 45, 50, 55, and 60 degrees with the depth of each wall angle of 5 mm was used. During the screening phase, the fifteen mixtures were firstly tested by using the achieved maximum wall angles without fracture as a criterion. Later on, the lubricant mixtures which could successfully form at the wall angle of 60 degrees with the forming depth of 20 mm would be tested in the stabilization phase to evaluate the formability and the forming temperature. The results showed that during the screening phase 11 lubricants could perform successfully, while the stabilization phase with the wall angle of 60 degrees only 3 lubricants could successfully form the workpiece. Therefore, this evaluation technique could help to evaluate and, for later on, be a criterion to select the suitable lubricant.

**Keywords**: Single-Point Incremental Forming (SPIF), Hot-dipped Zinc-coated Cold-rolled Steel, Lubrication condition, Percentage of thinning

## 1 Introduction

Single Point Incremental Forming (SPIF) process is a modern process for manufacturing a prototype and producing a small lot production [1]. This process is considered to be a dieless forming that can lower the overall production cost. Furthermore, it is highly flexible to form a complex product shape and capable of forming a low formability material, such as Titanium, Inconel and Bake Hardening Steels. The demand for producing more complex shapes and small lot quantities of sheet metals make the SPIF process be more attractive. However, the applications of the SPIF are still quite limited because it is extremely slow process and requires a complex machine (a CNC controlling machine). Therefore, efforts have been made to research to make it more practical for industries by increasing the production speed and the precision of product shapes and good surface finish. This would increase the opportunity to manufacture a large-scale production to serve wide ranges of the industries, such as automotive, biomedical device and aerospace [2]–[4].

The SPIF process deforms the sheet by using a half-spherical shape like a tool that moves along the plane (X-Y plane) with the defined contour path and the step depth (ΔZ) until acquiring the desired shape and depth as shown in Figure 1. The tool motion will cause of local plastic deformation at the contacting point. The forming force required is far less than that of a conventional sheet metal forming process, such as a stamping process, because of the small contacting area [1].

Many researchers have been studied to understand the process parameters affected the product quality. Durante *et al.* [5] identified and investigated influential factors that affect the formability and quality of the product as follows: 1) tool rotation speed (RPM), 2) feed rate, 3) step depth (ΔZ), 4) shape and size of the tool, 5) directions of the tool (for or against the tool rotation direction), and 6) friction at the tool-sheet interface. The rotational speed has direct effect on the contacting temperature and formability of the workpiece at the higher wall angles. The higher the rotational speed, the higher the contacting temperature and formability. Furthermore, he also conducted experiments to approximate the friction coefficient for rotational and non-rotational tools by measuring

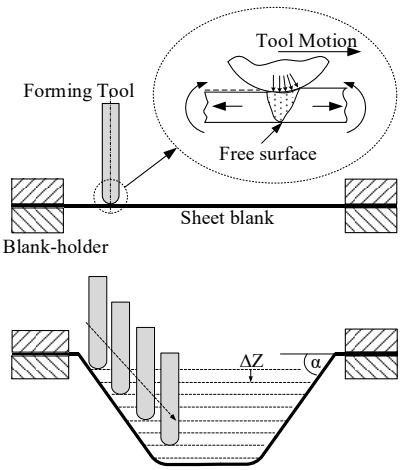


**Figure 1**: Schematic of Single Point Incremental Forming (SPIF) process [4].

the shear force and the normal force. According to the results, the friction coefficient of the rotational tool is much lower than that of the non-rotational too [6]. Kim and Park [7] applied Finite Element Modelling (FEM) to study the effect of the feed rates on the formability by using Forming Limit Curves (FLCs) as a fracture criterion of AA1050. The results showed that the formability could improve by lowering the feed rate. Another factor that could indicate the level of the formability of the material is the wall angel (α) as seen in Figure 1 because it is the direct impact on the wall thickness. In other words, when the wall angle exceeds 60 degrees, the product's wall thickness could be higher than 50% and produced uneven thickness distributions [8]. Therefore, the achieved wall angle could be used as the indicator to identify the level of the formability of the material after forming.

The direction of the tool and the step size (ΔZ) also influenced the formability, the surface quality and the level of the residual stress of the product. The direction of the tool could be for or against the direction of the tool. Most of the researchers recommend improving the surface quality by reducing the step size [9]–[16] using the against direction of the tool and selecting the suitable lubrication conditions [7]. For the suitable lubrication condition, the formability of the workpiece could be significantly improved by achieving the sliding friction condition at the interface between the workpiece and the tool. Furthermore, the feed

rate and the wall angle were the factors that directly affected lubrication conditions because they directly affected the contacting temperature. The heat under the sliding friction condition is generated as a thin film between the forming tool and the workpiece [17], [18]. However, this heat can be significantly reduced by a good lubricant and lubricating method [19], [20].

Currently, the lubricants have not yet been clearly defined in terms of what kind and which type of lubricant should be used and how it should be evaluated. Most of the time, the conventional lubricants used in sheet-forming processes, such as coconut oil or machining process, such as the mixing between the synthetic oil and coolant were employed. Also, the alternative lubricant, such as the mineral oil types were sometimes used because of the high viscosity at the high temperature. Therefore, it is of interest in deciding which lubricant is good for the SPIF process under different feed rates and tool rotation speeds especially in consideration of the formability of materials. Table 1 summarizes different types of lubricants, the feed rates and the tool rotation speeds used by many researchers.

**Table 1**: Summary of the lubricant types with different feed rates and tool rotation speeds studied by many researchers

| Lubricant Type | Researcher | Tool Totation Speed (rpm) | Feed Rate (mm/min) |
|---|---|---|---|
| Mineral Oil | Wei *et al.* [16] | 0 | 2600 |
| | Gupta and Jeswist [21] | 1000, 2000, 3000, 4000 | 3000, 4000, 5000, 7500 |
| | Adams and Jeswiet [22] | 25 | 1270 |
| | Dwivedey and Kalluri [23] | 700, 800, 900 | 300, 400, 500 |
| Forming Oil | Palumbo and Brandizzi [2] | 400, 1600 | 1800 |
| | Bagudanch *et al.* [24] | 1000 | 3000 |
| | Chang and Chen [26] | 1000, 4500, 6000 | 1500, 3500 |
| Coolant | Golabi and Khazaali [28] | 600 | 600 |
| Cutting oil | Silva *et al.* [27] | 35 | 1000 |
| $MoS_2$ | Xu *et al.* [25] | 100 | 2000 |
| | Chang and Chen [26] | 1000, 4500, 6000 | 1500, 3500 |

According to Table 1, different types, i.e., liquid oil, coolant, and solid lubricant, were used with a wide range of the tool rotational speed and feed rates. However, the cutting oil and coolant were used at a low rotational speed. The mineral and forming oils were frequently used with different ranges of the tool rotational speed ranges and feed rates. Wei *et al.* [16] tested the mineral oil without the tool rotation, while Adams and Jeswiet [21] defined tool rotation speeds at 25 rpm for the mineral oil. Dwivedey and Kalluri [22] used the tool rotation speeds at 700, 800, and 900 rpm, respectively. However, Gupta and Jeswiet [23] tried to apply the mineral oil at high tool rotation speeds of 1000–4000 rpm. Still, it is not successful at the tool rotation speeds over 3000 rpm because of the high temperature during the process. The smoke was observed during the test.

Forming oil type commonly used in the sheet metal forming process is employed by Bagudach *et al.* [24]. They successfully applied Houghton TD-52 as the lubricant with the tool rotation speed of 1000 rpm and the feed rate of 3000 mm/min.

Extreme Pressure (EP) lubricants in the form of liquid and solid were used and tested as well. Xu *et al.* [25] used $MoS_2$ lubricant to form Titanium TA1 with the tool rotational speed of 100 rpm with the feed rate of 2000 mm/min. Chang and Chen [26] studied the effect of the tool rotational speeds and the feed rate on the surface roughness. Solid lubricant, $MoS_2$, and liquid-based lubricant, rolling oil were used with two process variables, 1) tool rotation speeds as 1000, 4500 and 6000 rpm respectively and 2) feed rate as 1500 and 3500 mm/min.

Palumbo and Brandizzi [2] used lubricant in the hot metal forming group, OKS, at the elevated temperature incremental forming process of the car door shell with Ti6Al4V material by using electric static heating. Tool rotation speed of 400 and 600 rpm with the feed rate of 1800 mm/min were applied.

The lubricants in the machining process were also applied in the SPIF process. Silva *et al.* [27] used cutting oil as the lubricant to generate FLD of AA1050-H111 with the tool rotation speed of 35 rpm and the feed rate of 1000 mm/min. Golabi and Khazaali [28] studied the formability of SS304 by using coolants in machining a process as the lubricant with the tool rotation speed of 600 rpm and feed rate of 600 mm/min.

The important key parameter to improve the production rate for the SPIF process is to increase the feed rate. However, it will increase the friction between

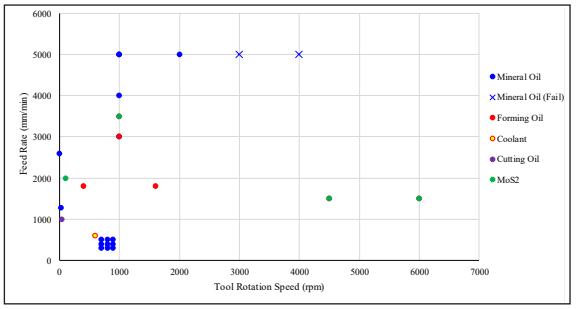


**Figure 2**: Lubricant types with different feed rates and tool rotational speeds' studies.

the tool and workpiece interface. Therefore, increasing the tool rotational speed allows the friction to be reduced. To reduce the effect of the friction and temperature further the proper lubricant is required. Unfortunately, no clear methods to justify the appropriate lubricants in the SPIF process at different process parameters are existed. Figure 2 shows the lubricant types from many researchers that applied in their works with different tool rotational speeds and feed rates. Roughly the lubricants are classified into 2 types; liquid lubricant and solid lubricant. Liquid lubricants are usually applied at the tool rotational speeds lower than 2000 rpm while the solid lubricant was used at the tool rotational speeds more than 2000 rpm.

Currently, no clear technique is used to characterize the lubricant. Thus, this research aimed to propose the systematic evaluation technique used only to evaluate the effect of the lubricants on the formability and the occurrence of the temperature. This technique is divided in two phases. The first would consider the possibilities of the lubricants to be performed at different wall angles (Formability evaluation), and the second considered the temperature stability during the process. The experiment was conducted with the lubricants used in the bulk-forming process in the form of 1) Solid and 2) Liquid base lubricants mixed with the coconut oil to adjust the viscosity at various ratios. The sheet material was a Hot-Dipped Zinc-coated cold roll steel, and the tests were performed with the mini-CNC. Tool rotation speeds of 2000 rpm and the feed rates of 1500 mm/min are classified in the medium to a high-speed range of the process that can apply for liquid and solid lubricants. The measurement results were the online temperature measurement, the maximum wall angle, the depth, and the thinning. These variables

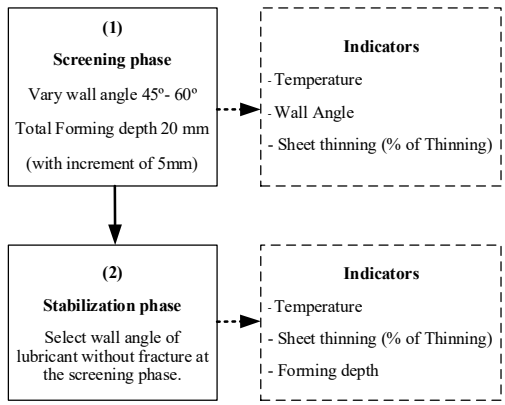


**Figure 3**: Experimental procedures for evaluating the performance of lubricants.

could evaluate the processes formability for selecting the proper lubricants for this process.

## 2 Materials and Methods

### 2.1 *Methodology (Experimental Procedure)*

The experiment was divided into 2 phases, as shown in Figure 3. First, the screening phase is to quickly evaluate the efficiency of the lubricants with many forming conditions via different wall angles but constant forming depth of 5 mm. While, second, the stabilization phase is to ensure the durability of the lubricants at the maximum wall angle condition for a long processing time.

#### *2.1.1 Screening phase*

The screening phase was conducted for lubricants by considering the level of the achieved maximum of wall angles. The workpiece was deformed in the frustum of a cone shape with the wall angle range from 45–60 degrees wall angle. The angle should be increased every 5 degrees at each forming depth of 5 mm. The overall depth of the specimen is 20 mm, as shown in Figure 4(a). The experiment started with the wall angle of 45 degrees. Then, the wall angle would incrementally increase 5 degrees for every 5 mm depth until reaching 60 degrees or else the sheet was fracture before. The measurement results are the temperature profile. The slopes of the temperature profile and the maximum temperature have a direct

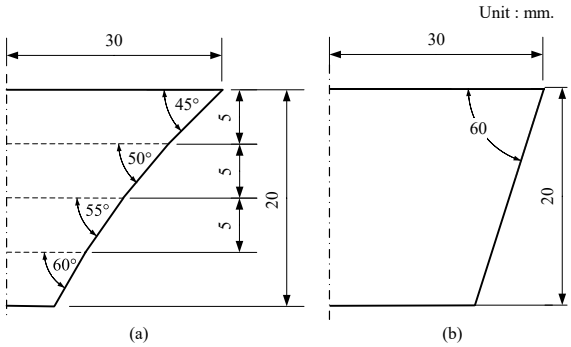


**Figure 4**: Shape and size of the specimen during; (a) screening phase performed with a wall angle range from 45–60 degrees, 5 mm increment depth for each wall angle, and (b) the stabilization phase conducted with a wall angle of 60 degrees and 20 mm maximum depth.

effect on the performance of lubricants. The highest wall angles indicate the formability and the deviation of the percentage of thinning of the finished workpiece at different wall angles when compared to the thersitical thinning obtained by the Sine's law.

*2.1.2 Stabilization phase*

The stabilization phase considers the durability of the lubricants that can perform throughout the whole process. During the long process, the lubricant will experience a high temperature which may deteriorate the viscosity and lubricity. Therefore, the lubricant must be evaluated. During the screening phase, the successful forming with the maximum wall angles in each lubricant was repeated again with that maximum wall angle with the 20 mm depth. However, in this study, only the successful lubricants performed at the maximum wall angle of 60 degrees were selected to repeat with the cup depth of 20 mm as shown in Figure 4(b) to demonstrate the durability of the lubricant. The temperature profile, the highest temperature, the percentage of thinning, and the maximum depth were measured. The specimen that could perform until the depth of 20 mm is considered to be a good lubricant.

## 2.2 *Approximation of the theoretical wall thickness by Sine's law*

One of the limitations in the SPIF process is the wall angle, which affects directly the thickness of the

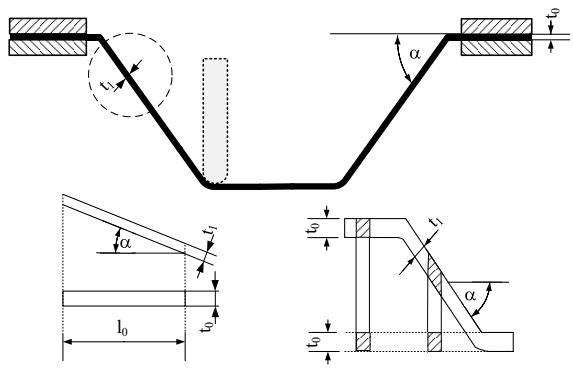


**Figure 5**: Schematic of Sine's laws for thickness approximation.

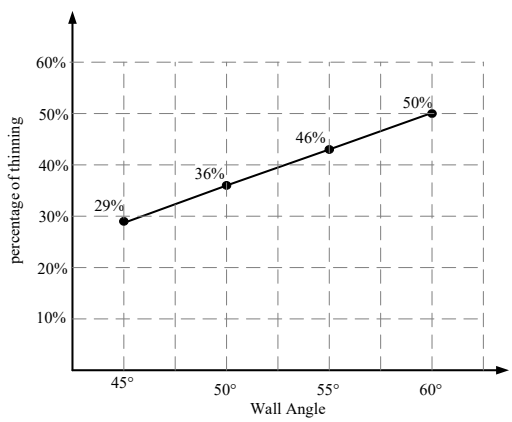


**Figure 6**: Percent thinning determined by the Sine's law with a wall angle range from 45 degrees to 60 degrees.

specimen with the assumption of the pure projection of surface element [29]–[31] as shown in Figure 5. The sine's law estimates the theoretical sheet thickness ($t_1$) from the initial sheet thickness ($t_0$). The function has a variable of the wall angle ($\alpha$) as shown the Equation (1). Sine's law considers only the dimensional changes, not the minor strain as seen in Figure 5.

$$t_1 = t_0 \sin\left(\frac{\pi}{2} - \alpha\right) \quad (1)$$

The specimen's wall angles are in the range from 45 degrees to 60 degrees with 5 degrees incrementally which can approximate different thicknesses. The percentage of thinning was determined by Equation (2) as shown in Figure 6. At 60 degrees, the percent thinning is around 50% which is considered to be the maximum thinning most of the materials can be achieved at the

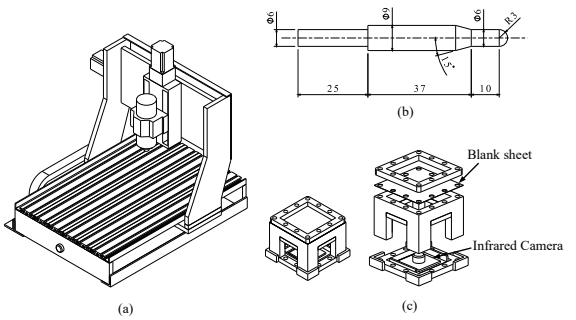


**Figure 7**: Machine, forming tool and fixtures for SPIF process; (a) Mini-CNC model LY 3040 (b) Forming tool, and (c) Fixture and infrared camera.

room temperature. Therefore, the wall angle exceeded 60 degrees were critical for this forming process.

$$\text{percentage of thinning} = \frac{\text{initial thickness}(t_0) - \text{thickness}(t_1)}{\text{initial thickness}(t_0)} \quad (2)$$

## 2.3 *Experimental details*

### *2.3.1 Materials*

Hot-Dipped Zinc-Coated cold-rolled steel sheet, SGCH grade manufactured based on the standard TIS.50-2548 was used in this study [32]. The chemical composition is shown in Table 2. The sheet was coated based on Cold Rolled Carbon Steel Sheets and Strip (SPCC) according to JIS G3141 [33].

**Table 2**: Chemical Compositions (Wt%) of SPCC

| Steel | C | Mn | P | S |
|---|---|---|---|---|
| SPCC | 0.15 | 0.60 | 0.10 | 0.05 |

### *2.3.2 SPIF tooling*

The forming machine was Mini CNC Model LY 3040 as shown in Figure 7(a), with a maximum feed rate of 1500 mm/min. The spindle motor is 800 W with the rotational speed in the range of 0–24,000 rpm. The forming tool is made of a S55C half-spherical tip with a surface hardening and the diameter of 6 mm as shown in Figure 7(b). The fixture was designed to clamp four sides of the specimen, and the infrared camera to measure the temperature was installed at the lower part of the die as illustrated in Figure 7(c).

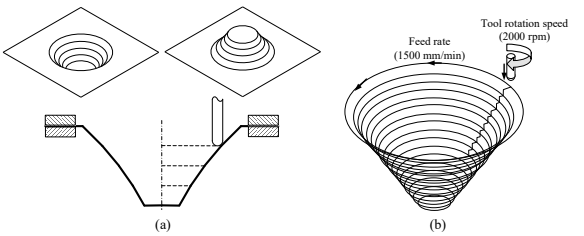


**Figure 8**: Tool and workpiece conditions; (a) the clamp holder at the four sides of the specimen and (b) the directions of the tool rotation and feed.

### *2.3.3 Operating conditions*

The operating parameters were the tool rotation speed, the feed rate, the tool path, and the step size (Δz). The tool rotational direction was set with the clockwise direction with the rotational speed of 2000 rpm and the tool path direction was defined with the counterclockwise direction with a feed rate of 1500 mm/min as shown in Figure 8. The step depth is 0.2 mm. The maximum depth forming (H) is 20 mm. All of the process parameters are presented in Table 3.

**Table 3**: Process parameters

| Parameter | Value |
|---|---|
| 1. Tool rotation direction | Clockwise |
| 2. Tool rotation speed, ω (rpm) | 2000 |
| 3. Tool diameter, $d_t$ (mm) | 6 |
| 4. Tool direction | Counterclockwise |
| 5. Feed rate, f (mm/min) | 1500 |
| 6. Step Size, ΔZ (mm) | 0.2 |
| 7. Forming Depth, H (mm) | 20 |

### *2.3.4 Temperature measurement technique*

The measurement of temperature was moderately difficult, because the contact area between the forming tool and the specimen is small and constant movement. Therefore, to use a direct-contact device on the workpiece, such as a thermocouple, placed behind the specimen to record the temperature would make it difficult to monitor the thermal area continuously throughout the process. Therefore, the infrared camera was utilized to measure the distributions of heat. The experiment was arranged and prepared with the infrared camera (IR camera), Flir lepton 3.5 radiometry long-wave infrared camera module and installed on the basement

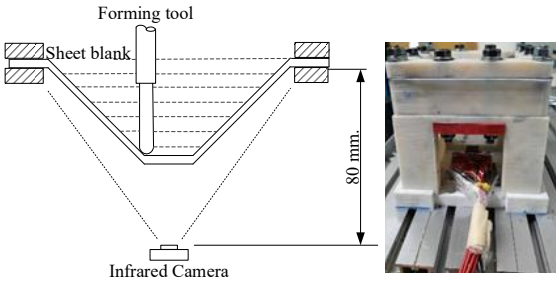


**Figure 9**: Position of the infrared camera to measure the temperature.

of the fixture as seen in Figure 7(c). The measurement is done perpendicular to the specimen by detecting the heat distributions online during the forming process as seen in Figure 9.

The setting criterion of the infrared are the distance between the camera and specimen which is controlled at the constant displacement. The highest temperature was recorded online during the process.

*2.3.5 Specimen geometry measurement*

Specimen geometry obtained from the experiment was measured in 2 parts as shown in Figure 10; 1) the thickness (t) of the specimen at the maximum depth and 2) the highest depth, which is used to determine the formability (Maximum of depth forming; Hmax). The wall thickness (t) is measured at the wall of the specimen in the deepest zone as shown in Figure 10 by a point-to-point micrometer (specification: measuring range 0–25 mm, instrument error 0.002 mm with a minimum display of 0.001 mm). The highest depth (Hmax, Maximum of depth forming) was measured directly from the displayed of the Mini-CNC at the last position of the forming tool without specimen fracture. In the condition of the fracture specimen, the value, when the damage occurred, was also measured.

*2.3.6 Lubrication conditions*

The principal of the SPIF process is a point contact between the tool and the workpiece. This circumstance may generate extremely high temperature and high contact friction right at the contact area, directly affecting the forming force. If the friction is high enough, the tool can hold the workpiece at the contact, which causes the extensive pull force to elongate the adjacent

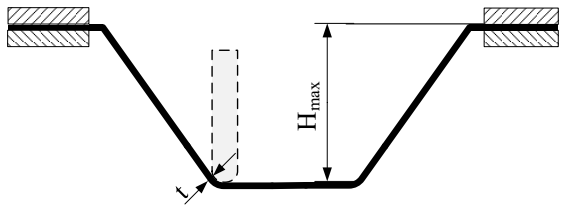


**Figure 10**: Position to measure the thickness of the specimen.

material. As a result, the neighbor area may experience the excessive thinning. Therefore, to apply the proper lubricants is essential to control the appropriate tribological condition, which affects the forming force, temperature, and surface quality. Lubricants of the metal forming process are the first idea to apply in SPIF process especially the lubricants can resist Extreme Pressure (EP). Tavichaiyuth *et al.* [34] successfully used the solid lubricant, graphite mixed with water (graphite 5% by volume), as the lubricant in the hot forging process to form axle shaft. Sae-eaw and Aue-u-lan [35] applied the liquid base lubricant, namely Calform NF 206 in the ball ironing testing. The result found that Calform NF 206, performs the same as the Zn-Ph coating, normally used in the cold forging process. Therefore, in this research, the graphite base and Calform NF 206 were selected as the main lubricants and they were also mixed with the coconut oil to adjust the viscosity of the lubricant mixtures. The coconut oil is a suitable solvent and lubricity for both graphite and Calform NF 206, easy to use and can be performed as a cooling agent.

Table 4 shows the property of each lubricant, and Table 5 summarizes all the lubrication conditions. Each lubricant was applied by flooding at the center of the workpiece with the amount of 150 mL.

## 3 Results and Discussion

The experiment was arranged and prepared to characterize the lubricant via 2 phases, as shown in Figure 3. The results are presented as follows:

### 3.1 *Screening phase*

The screening was done to determine initially what kind of lubricant was usable based on the maximum wall angle. The specimens were tested with the wall

**Table 4**: Properties of the lubricants

| Type | Commercial Code | Detail | |
|---|---|---|---|
| Media | Coconut Oil | Kinetic viscosity at 40 °C ($mm^2/s$) | 40.6 |
| | | Kinetic viscosity at 100 °C ($mm^2/s$) | 8.2 |
| | | VI Index<br>Flashpoint temperature (°C) | 182<br>180 |
| Solid lubricant | MGF 4 995 | Carbon content (in % C) | >95.5 |
| | | Particle size | d50 3–5.5 μm |
| Liquid-based | Callington Calform NF206 | Density at 30 °C ($g/mm^3$) | 0.934 |
| | | Kinetic viscosity at 40 °C ($mm^2/s$) | 480 |
| | | Kinetic viscosity at 100 °C ($mm^2/s$) | 32.2 |
| | | VI index | 98 |
| | | Rotational viscosity at 6 rpm (mPa·s) | 1000 |
| | | Rotational viscosity at 60 rpm (mPa·s) | 1425 |
| | | Flashpoint temperature (°C ) | 210 |

**Table 5**: Lubrication conditions used in this study

| Group of Lubricant | Lubricant Code | Details (Mixed Ratio) |
|---|---|---|
| A : Media | Lub a | Pure of Coconut Oil |
| B : Solid + Media | Lub b-1 | Graphite + Coconut Oil (2.5 : 1) |
| | Lub b-2 | Graphite + Coconut Oil (2 : 1) |
| | Lub b-3 | Graphite + Coconut Oil (1 : 1) |
| | Lub b-4 | Graphite + Coconut Oil (1 : 2) |
| | Lub b-5 | Graphite + Coconut Oil (1 : 3) |
| | Lub b-6 | Graphite + Coconut Oil (1 : 5) |
| | Lub b-7 | Graphite + Coconut Oil (1 : 8) |
| C : Liquid-based + Media | Lub c-1 | Pure of Callington Calform NF-206 |
| | Lub c-2 | Callington Calform NF-206 + Coconut Oil (1 : 1) |
| | Lub c-3 | Callington Calform NF-206 + Coconut Oil (1 : 2) |
| | Lub c-4 | Callington Calform NF-206 + Coconut Oil (1 : 3) |
| | Lub c-5 | Callington Calform NF-206 + Coconut Oil (1 : 5) |
| | Lub c-6 | Callington Calform NF-206 + Coconut Oil (1 : 8) |
| | Lub c-7 | Callington Calform NF-206 + Coconut Oil (1 : 10) |

angle in the range of 45 degrees to 60 degrees as seen in Figure 4(a). The performance was evaluated by the highest generated temperature, the highest wall angle, and the percent thinning of the finished specimen.

### *3.1.1 Effect of temperature*

Location of the high-temperature region is observed with the bright shades of yellow, orange, red, purple, blue, and black, respectively. The yellow shade is represented the highest temperature. The thermogenesis was comet shape-like moving along the position of the tool, as shown in Figure 11. The highest temperature has occurred right at the contacting positions between the forming tool and specimen. Then, the temperature was dropped gradually after the forming tool passed.

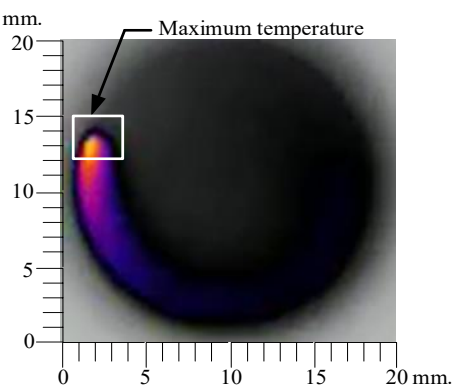


**Figure 11**: Measurement of temperature distributions by the infrared camera.

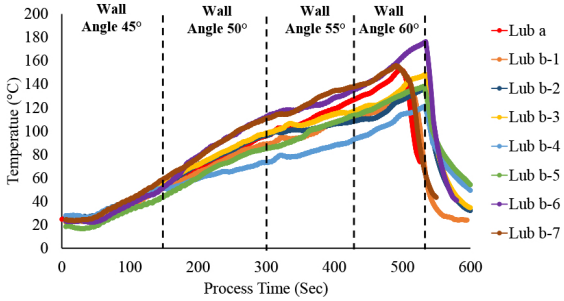


**Figure 12**: Temperature profiles in the screening phase of the solid + media (group b) lubricants.

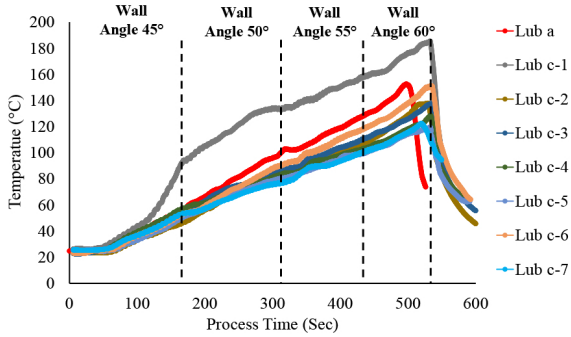


**Figure 13**: Temperature profiles during the screening phase of the liquid-based + media (group c) lubricants.

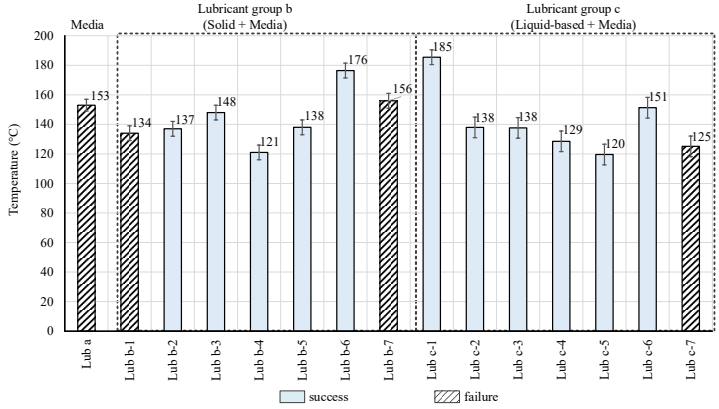


**Figure 14**: Highest temperature measurement during the screening phase for each lubricant.

According to Figures 12 and 14, the pure coconut oil (Lub a) was failed at the maximum wall angle to 60 degrees, and the temperature increased gradually to 153 °C. Then, the graphite (solid lubricant) was mixed with the coconut oil at different ratios. Only two lubricants in the group cannot form the parts successfully. Lub b-1 has the highest graphite concentration (thick mixture), so it is difficult to be mixed homogeneously. As a result, the thin film layer was hard to penetrate between the tool and the workpiece. However, the temperature profile for all fail cases (Lub b-1 and Lub b-7) was similar to the successful conditions. The maximum temperature in Lub b-1 and Lub b-7 is 134 °C and 156 °C, respectively. Even though Lub b-7 has a much less concentration of Lub b-1, the maximum temperature of Lub b-7 is higher than that of Lub b-1 because the amount of graphite is much less, which cannot provide enough lubricant to reduce friction. For other cases in this group, the parts were successfully formed at the 60 degrees, and the maximum temperature is in the range between 121 °C to 176 °C . It indicates that when applying the solid lubricant, the level of concentration (ratio between solid lubricant and media) is important to provide enough lubricity and control the maximum temperature.

Figures 13 and 14 show the results of the Calform NF 206 mixed with the coconut oil at different ratios. This group is called liquid based lubricants. Calform NF 206 is easy to mix with the coconut oil homogeneously. Only Lub c-7 cannot successfully form the part, because as mentioned before, in the solid lubricant group, the amount of lubricant is not enough to reduce the friction. The rest conditions can form the part at the wall angle of 60°. The highest temperature of 185 °C happened with the pure Calform NF 206, and also the rate of increasing temperature, see Figure 13, is also high. The part in this condition can still successfully

form. This can be explained by the fact that this lubricant is very good to reduce friction, but the viscosity is very high. Therefore, it is hard to a generate thin film between the tool and the workpiece. When Calform NF 206 mixed with the coconut oil, it reduces the viscosity, which can help the lubricant to generate the thin film between the tool and workpiece. As a result, the maximum temperature is in the range of 120–138 °C, and also the temperature is gradually increased. Therefore, the ratios of the mixed lubricant are important factors to form the part successfully.

According to the results during the screening phase, the maximum temperature is not significant to evaluate the efficiency of lubricants due to a short processing time at the severe condition (high wall angle).

### *3.1.2 Effect of wall angle*

The degree of the wall angles in this research is used to evaluate the performance of the lubricants. As seen in Figure 15, the wall angle will affect the level of the frictional force because the contacting surface area between the workpiece and the tool shown in Equation (3) increases when the wall angle increases. Therefore, $F_t$ (reaction force at the contacting point) will be changed by the degree of the wall angle. The Fty is a resisted force against the tool's direction. If the wall angle is higher, the frictional force is also higher. The wall angles of 45, 50, 55, and 60 degrees with the depth of each wall angle of 5 mm was defined for the screening phase to indicate different degrees of the friction conditions by ascending of the frictional force.

$$d_{max} = r\sqrt{2(1-\cos(2\alpha)} \quad (3)$$

$d_{max}$ = Maximum tool diameter that contacted the workpiece at point a (mm)
$r$ = Tool radius (mm)
$\alpha$ = Wall angle (Degree)

These experiments were conducted by varying the lubricant types with the fixed tool rotation speed of 2000 rpm, feed rate of 1500 mm/min, and step size of 0.2 mm. According to Figure 16, all the unsuccessful cases for both solid and liquid-based lubricants can perform up to the maximum wall angle of 55 degrees, but they also can deform at 60 degrees with the depth less than 5 mm. The unsuccessful conditions happen for the rich mixture of the solid lubricant (Lub b-1)

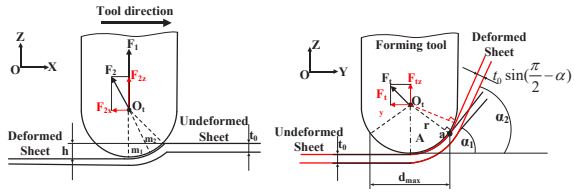


**Figure 15**: Free-body diagram of the contacting point between the tool and the specimen at different planes.

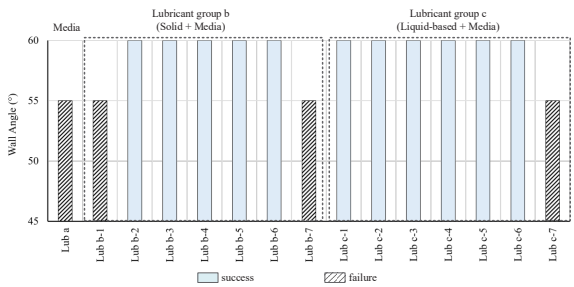


**Figure 16**: Highest wall angle formed during the screening phase for each lubricant.

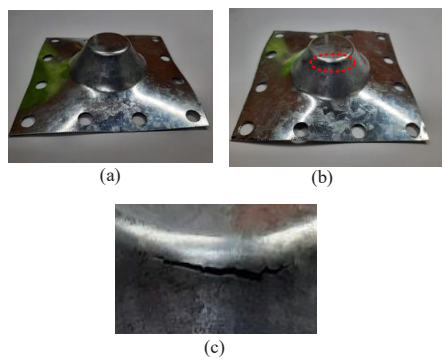


**Figure 17**: Examples of specimens during the screening phase; (a) successful part (b) failure part (c) zoom-in the location of the fracture.

and less mixture of both solid and liquid lubricants (Lub b-7 and Lub c-7). The fracture location was happened at the circumference adjacent to the tool as shown in Figure 17. This indicates that at the severe condition (60 degrees wall angle) with the rich and weak mixtures for the solid and liquid lubricants they cannot generate enough thin film to lubricate the workpiece during the process. All the successful conditions during the screening phase were repeated in the stabilization phase with the condition of 60 degrees wall angle and 20 mm depth.

### *3.1.3 Effect of sheet thinning*

The thickness of the specimen was recorded at the highest depth and compared with the theoretical thinning determined by the Sine's law. The results are presented in terms of the percentage of thinning, as summarized in Table 6. The initial thickness of the specimen is 0.176 mm. Sine's law estimates the thickness with the highest depth of 60 degrees equal to 0.088 mm and the percentage of thinning of 50%. According to Figure 18, the successful forming cases with good lubricants can provide the thinning were around 50% in which is closed to the Sine's law approximation. On the other hand, the fracture specimens give the maximum thinning, which is higher than the approximation by 2–3%.

The thickness strain calculated from the Sine's law is ideal. It is fundamentally a function of geometrical parameters but not of friction. However, in practice, the lubrication conditions are by far important to form material successfully. In the incremental forming process, the tool will contact the workpiece continuously during the process. If the lubrication condition is not good enough, it is difficult to maintain the thinning in accordance with the Sine's law.

## 3.2 *Stabilization phase*

The stabilization phase was continued to further evaluate the performance of the successful lubricants during the screening phase, which will deform with the wall angle of 60 degrees. The performance was evaluated by the measurement of the highest generated temperature, the highest forming depth, and the percentage of thinning of the finished specimen as shown in Table 7.

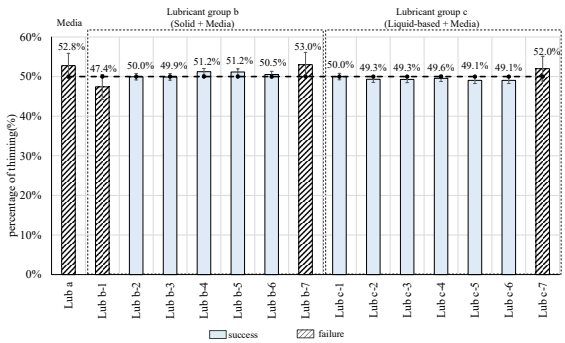


**Figure 18**: Percent thinning at the highest depth of lubricants during the screening phase and compared with the thinning approximated by the Sine's law.

### *3.2.1 Effect of temperature*

The testing condition employed with the high tool rotational speed and the maximum wall angle resulting in the high generated temperature due to the high friction. This severe condition would elaborate and extract the extreme performance of lubricants at the

**Table 6**: Results of the screening phase for various lubricants

| Lubricant | Average Max Temperature (°C) | Highest Wall Angle can Form | Average Thickness of Wall (mm) | Percentage of Thinning (%) | Different of percentage of Thinning form Sine's law | Formability |
|---|---|---|---|---|---|---|
| Lub a | 153 | 55° | 0.084 | 52.8% | 2.8% | Failure |
| Lub b-1 | 134 | 55° | 0.092 | 47.4% | –2.6% | Failure |
| Lub b-2 | 137 | 60° | 0.088 | 50.0% | 0.0% | Success |
| Lub b-3 | 148 | 60° | 0.088 | 49.9% | –0.1% | Success |
| Lub b-4 | 121 | 60° | 0.087 | 51.2% | 1.2% | Success |
| Lub b-5 | 138 | 60° | 0.086 | 51.2% | 1.2% | Success |
| Lub b-6 | 176 | 60° | 0.087 | 50.5% | 0.5% | Success |
| Lub b-7 | 156 | 55° | 0.082 | 53.0% | 3.0% | Failure |
| Lub c-1 | 185 | 60° | 0.088 | 50.0% | 0.0% | Success |
| Lub c-2 | 138 | 60° | 0.089 | 49.3% | –0.7% | Success |
| Lub c-3 | 138 | 60° | 0.090 | 49.3% | –0.7% | Success |
| Lub c-4 | 129 | 60° | 0.089 | 49.6% | –0.4% | Success |
| Lub c-5 | 120 | 60° | 0.090 | 49.1% | –0.9% | Success |
| Lub c-6 | 151 | 60° | 0.090 | 49.1% | –0.9% | Success |
| Lub c-7 | 125 | 55° | 0.085 | 52.0% | 2.0% | Failure |

**Table 7**: Experimental results of the lubricants during stabilization

| Lubricant | Max Temperature (°C) | Forming Depth (mm) | Thickness of Wall (mm) | Percentage of Thinning (%) | Different of percentage of Thinning from Sine's law | Formability |
|---|---|---|---|---|---|---|
| Lub b-2 | 127 | 5.6 | 0.081 | 53.9% | 3.9% | failure |
| Lub b-3 | 117 | 8.6 | 0.082 | 53.3% | 3.3% | failure |
| Lub b-4 | 114 | 6.2 | 0.082 | 53.3% | 3.3% | failure |
| Lub b-5 | 129 | 5.4 | 0.081 | 54.0% | 4.0% | failure |
| Lub b-6 | 135 | 5.2 | 0.078 | 55.6% | 5.6% | failure |
| Lub c-1 | 121 | 8.4 | 0.073 | 58.3% | 8.3% | failure |
| Lub c-2 | 107 | 20 | 0.087 | 50.5% | 0.5% | success |
| Lub c-3 | 116 | 20 | 0.087 | 50.7% | 0.7% | success |
| Lub c-4 | 127 | 20 | 0.090 | 48.6% | -1.4% | success |
| Lub c-5 | 127 | 6.8 | 0.077 | 56.3% | 6.3% | failure |
| Lub c-6 | 150 | 5.4 | 0.087 | 55.6% | 5.6% | failure |

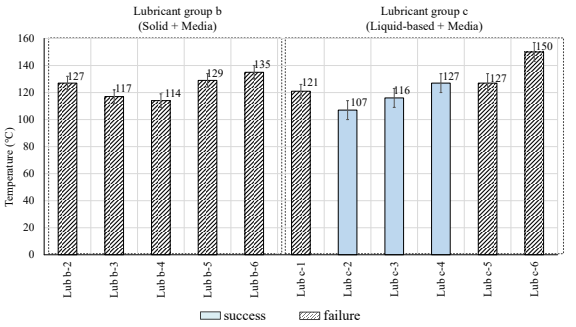


**Figure 19**: Highest temperature and forming depth with the SPIF process during the stabilization phase.

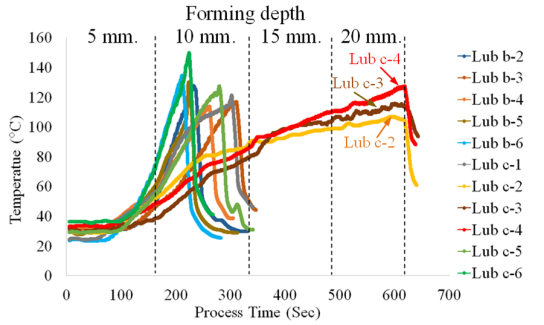


**Figure 20**: Temperature profiles during the stabilization phase for each lubricant.

high potential production rate. According to Figure 19, all the solid lubricant conditions were failed during the tests. The maximum temperature was in the range of 127 to 135 °C . Even though the level of the maximum temperature is not high, the rate of increasing temperature see Figure 20 is extremely high. This may be due to the the broken down the lubricant film during the test. For the liquid-based lubricant, only Lub c-2, Lub c-3, and Lub c-4, which have the highest temperatures of 107 °C, 116 °C and 127 °C, respectively are successful as seen in Figure 19.

Figure 20 presents the temperature profile of all the testing conditions during the stabilization phase. At the early phase, every lubricant had a similar tendency of temperature considered by the degree of the slope. The successful lubricants, Lub c-2, Lub c-3, and Lub c-4, had a gradual increase tendency of the temperature until the finished process. For the unsuccessful group, the tendency to increase the temperature was rapid until the workpiece fractures caused by the unstable friction in the process. When considering the maximum temperature although Lub c-4 and Lub c-5 generated the same temperature level, Lub c-5 could not successfully form the part. This evidence showed that the temperature didn't significantly affect the formability. In other words, low or high temperature does not indicate success in forming. It can be concluded that the proper lubricants in the SPIF process, in addition to the main role of reducing the friction, must have a function to cool down the tool and workpiece due to high tool rotation speed. The good lubricants must be able to maintain the temperature gradually increasing throughout the process.

### *3.2.2 Effect of the forming depth*

The successful specimen has the forming depth of 20 mm, as shown in Figure 21(a). The failure specimens

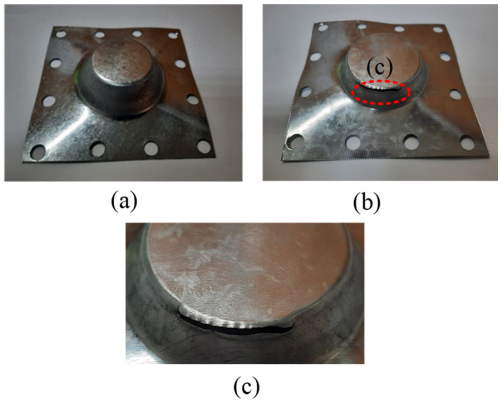


**Figure 21**: Specimen during the stabilization phase, (a) the successful specimen, and (b) the failure specimen in the stabilization phase (c) zoom-in the location of the fracture.

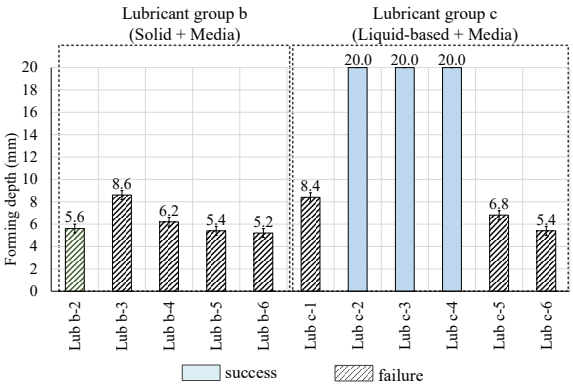


**Figure 22**: Forming depth of the specimens during the stabilization phase for each lubricant.

were fractured with the depth in the range from 5–10 mm, while the successful specimens can reach up to 20 mm depth. Figure 21(b), (c), and Figure 22 show the fracture specimen and achieved forming depth for all conditions, respectively. For the fracture specimens, the fracture happens adjacent to the tool because the workpiece's wall was sticked to the tool and pulled to elongate the neighbouring workpiece's wall generating the excessive wall thinning, see Figure 21(c).

*3.2.3 Effect of thinning on the sheet*

The specimen was a frustum cone with a wall angle of 60 degrees, which has approximated percentage of wall thinning of 50%, closed to Sine's law approximate. The

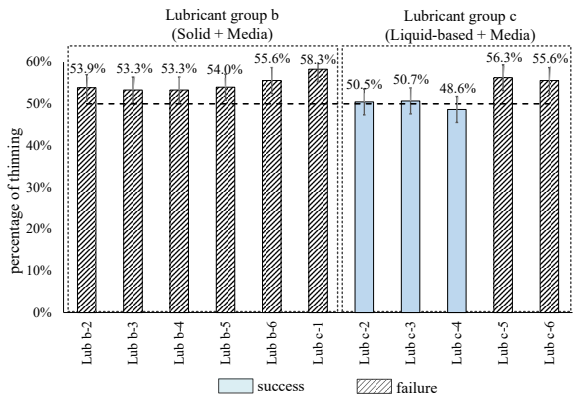


**Figure 23**: Percentage thinning at the highest position and compared with Sine's law at 60 degrees wall the angle of different lubricants during the stabilization phase.

percentage of the thinning for the successful specimen was 48.6–50.7%. The failure specimen differed from approximation by more than 3%, as shown in Figure 23. The thinning of the sheet from the SPIF process when assessed with the Sine's law, the percentage of thinning was calculated by the geometry, which an ideal case of the deformation.

**Nomenclature**

$\alpha$ = Wall Angle
$\omega$ = Tool Rotation Speed
$d_t$ = Tool diameter
f = feed rate
$\Delta z$ = Step Size
H = Forming depth
$t_0$ = Initial Sheet Thickness
t = thickness of wall

## 4 Conclusions

A lubricant evaluation technique provided a guideline for the selection of lubricants to be used in SPIF Process. The techniques to characterize the lubricants was divided into 2 phases; 1) the screening phase and 2) the stabilization phase. The screening phase is quick and easy to determine the performance of the lubricants by using the highest wall angle. The stabilization phase is used to determine the stability of the lubricants at the highest wall angles. The rate of increasing temperature not the maximum

temperature, can indicate the performance of the lubricant.

To evaluate the lubricant used in SPIF by using both phases to ensure the successful process. The main advantage of this technique can be recognized in terms of the economic that the number of samples for this technique can be minimized, especially during the screening phase before moving on to the stabilization phase.

**References**


[1] R. Aerens, P. Eyckens, A. Van Bael, and J. R. Duflou, "Force prediction for single point incremental forming deduced from experimental and FEM observations," *The International Journal of Advanced Manufacturing Technology*, vol. 46, pp. 969–982, 2010.

[2] G. Palumbo and M. Brandizzi, "Experimental investigations on the single point incremental forming of a titanium alloy component combining static heating with high tool rotation speed," *Material and Design*, vol. 40, pp. 43–51, 2012.

[3] J. R. Duflou, A. K. Behera, H. Vanhove, and L. S. Bertol, "Manufacture of accurate titanium cranio-facial implants with high forming angle using single point incremental forming," *Key Enginerring Materials*, vol. 549, pp. 223–230, 2013.

[4] J. Jeswiet, J. R. Duflou, and A. Szekeres, "Forces in single point and two point incremental forming," *Advanced Materials Research*, vol. 6–8, pp. 449–456, 2005.

[5] M. Durante, A. Formisano, A. Langella, and F. M. C. Minutolo, "The influence of tool rotation on an incremental forming process," *Journal of Materials Processing Technology*, vol. 209, pp. 4621–4626, 2009.

[6] G. Buffa, D. Campanella, R. Mirabile, and L. Fratini, "Improving formability in SPIF processes through high-speed rotating tool: Experimental and numerical analysis," *Key Engineering Materials*, vol. 549, pp. 156–163, 2013.

[7] Y. Kim and J. Park, "Effect of process parameters on formability in incremental forming of sheet metal," *Journal of Materials Processing Technology*, vol. 130–131, pp. 42–46, 2002.

[8] D. Xu, B. Lu, T. Cao, J. Chen, H. Long, and J. Cao, "A comparative study on process potentials for frictional stir and electric hot assisted incremental sheet forming," *Procedia Engineering*, vol.81, pp. 2324–2329, 2014.

[9] A. Attanasio, E. Ceretti, and C. Giardini, "Optimization of tool path in two points incremental forming," *Journal of Materials Processing Technology*, vol. 177, pp. 409–412, 2006.

[10] B. V. Desai, K. P. Desai, and H. K. Raval, "Die-less rapid prototyping process: Parametric investigations," *Procedia Materials Science*, vol. 6, pp. 666–673, 2014.

[11] J. R. Patel, K. S. Samvatsar, H. P. Prajapati, and U. M. Sharma, "Analysis of variance for surface roughness produced during single point incremental forming process," *International Journal of New Technologies in Science and Engineering*, vol. 2, pp. 90–97, 2015.

[12] S. Kurra and S. Regalla, "Multi-objective optimization of single point incremental sheet forming using Taguchi-based grey relational analysis," *International Journal of Materials Engineering Innovation*, vol. 6, pp. 74–90, 2015.

[13] P. B. Uttarwar, S. K. Raini, and D. S. Malwad, "Optimization of process parameter on surface roughness (Ra) and wall thickness on SPIF using Taguchi method," *International Research Journal of Engineering and Technology*, vol. 2, no. 9, pp. 781–784, 2015.

[14] R. Jagtap, S. Kashid, S. Kumar, and H. M. A. Hussein, "An experimental study on the influence of tool path, tool diameter and pitch in single point incremental forming (SPIF)," *Advances in Materials and Processing Technologies*, vol. 1, no. 3–4, pp. 465–473, 2015.

[15] D. S. Malwad and V. M. Nandedkar, "Deformation mechanism analysis of single point incremental sheet metal forming," *Procedia Materials Science*, vol. 6, pp. 1505–1510, 2014.

[16] H. Wei, G. Hussain, A. Iqbal, and Z. P. Zhang, "Surface roughness as the function of friction indicator and an important parameters-combination having controlling influence on the w: Resent results in incremental forming," *The International Journal of Advanced Manufacturing Technology*, vol. 101, pp. 2533–2545, 2019, doi: 10.1007/s00170-018-3096-1.

[17] J. A. Schey, "Tribology in metal working friction,

lubrication and wear," in *American Society for Metals*. Ohio: Metals Park, 1984, pp. 16–21.

[18] C. Xu, Y. Li, Z. Wang, Z. Cheng, and F. Liu, "The influence of self-lubricating coating during incremental sheet forming of TA1 sheet," *The International Journal of Advanced Manufacturing Technology*, vol. 110, pp. 2465–2477, 2020.

[19] B. Lu, Y. Fang, D. K. Xu, J. Chen, H. Ou, N. H. Moser, and J. Cao, "Mechanism investigation of friction-related effects in single point incremental forming using a developed oblique roller-ball tool," *International Journal of Machine Tools and Manufacture*, vol. 85, pp. 14–29, Oct. 2014.

[20] D. Xu, W. Wu, R. Malhotra, J. Chen, B. Lu, and J. Cao, "Mechanism investigation for the influence of tool rotation and laser surface texturing (LST) on formability in single point incremental forming," *International Journal of Machine Tools and Manufacture*, vol. 73, pp. 37–46, 2013.

[21] D. Adams and J. Jeswiet, "Single-point incremental forming of 6061-T6 using electrically assisted forming methods," *Proceedings of the Institution of Mechanical Engineers, Part B: Journal of Engineering Manufacturing*, vol. 228, no. 7, pp. 757–746, 2014.

[22] M. Dwivedy and V. Kalluri, "The effect of process parameters on forming forces in single point incremental forming," *Procedia Manufacturing*, vol. 29, pp. 120–128, 2019

[23] P. Gupta and J. Jeswiet, "Effect of temperatures during forming in single point incremental forming," *The International Journal of Advanced Manufacturing Technology*, vol. 95 pp. 3693–3706, 2018.

[24] I. Bagudanch, G. Centeno, C. Vallellano, and M. L. Garcia-Romeu, "Forming force in single point incremental forming under different bending conditions," *Procedia Engineering*, vol. 63, pp. 354–360, 2013

[25] C. Xu, Y. Li, Z. Wang, Z. Cheng, and F. Liu, "The influence of self-lubricating coating during incremental sheet forming of TA1 sheet," *The International of Advanced Manufacturing Technology*, vol. 110, pp. 2465–2477, 2020

[26] Z. Chang and J. Chen, "Analytical model and experimental validation of surface roughness for incremental sheet metal forming parts," *International Journal of Machine Tools and Manufacture*, vol 146, p. 103453, 2019

[27] M. B. Silva, P. S. Nielsen, N. Bay, and P. A. F. Martins, "Failure mechanism in single-point incremental forming of metals," *International Journal Advance Manufacturing Technology*, vol. 56, pp. 893–903, 2011.

[28] S. Golabi and H. Khazaali, "Determining frustum depth of 304 stainless steel plates with various diameters and thicknesses by incremental forming," *Journal of Mechanical Science and Technology*, vol. 28, no. 8, pp. 3273–3278, 2014.

[29] T. Altan and A. E. Tekkaya, "Incremental sheet forming" in *Sheet Metal Forming Process and Applications*. Ohio: ASM International Material Park, 2012, pp. 273–288.

[30] J. Jeswiet, F. Micari, G. Hirt, A. Bramley, J. Duflou, and J. Allwood, "Asymmetric single point incremental forming of sheet metal," *CIRP Annals*, vol. 54, pp. 623–649, 2005.

[31] J. Jeswiet, D. Adams, M. Doolan, T. McAnulty, and P. Gupta, "Single point and asymmetric forming," *Advance Manufacture*, vol. 3, pp. 253–262, 2015.

[32] *Hot-Dip Zinc-Coated Cold-Rolled Steel Coil, Sheet and Corrugated Sheet*, TIS 50-2548, Nov. 2005.

[33] *Cold-reduced Carbon Steel Sheets and Strips*, JIS G 3141, 2005.

[34] C. Tavichaiyuth, Y. Aue-u-Lan, and T. Hart-Rawung, "Evaluation of forging die defect by considering plastic deformation and abrasive wear in a hot forged axle shaft," *Applied Science and Engineering Progress*, vol. 14, no. 1, pp. 60–71, 2021, doi: 10.14416/j.asep.2020.12.005.

[35] N. Sae-eaw and Y. Aue-u-lan, "Friction evaluation for combined drawing and ironing process with thick sheet by ball ironing," *Journal of Manufacturing Science and Engineering*, vol. 143, 2020, Art. no. 061004.